Proceedings of the International Conference on Industrial Engineering and Operations Management

Publisher: IEOM Society International, USA DOI: 10.46254/BA08.20250233
Published: December 20, 2025

Back-Pressure Effects on Shock Waves in a Conical CD Nozzle: An Analytical and CFD Study

MD Abdullah AR Rifat
Mechanical Engineering Department
Chittagong University of Engineering and Technology
Chattogram, Bangladesh
mdabdullaharrifat123@gmail.com

Forhad Hossain
Mechanical Engineering Department
Chittagong University of Engineering and Technology
Chattogram, Bangladesh
forhadhossan232@gmail.com

Amit Chandra Day
Mechanical Engineering Department
Chittagong University of Engineering and Technology
Chattogram, Bangladesh
amitchandradey17@gmail.com

Abstract

An ideal converging-diverging (CD) nozzle accelerates a subsonic flow to supersonic by converging the flow to sonic speed at the throat and diverging it until supersonic speed is reached. Such nozzles are commonly employed in rocket engines, where the primary objective is to convert pressure energy into kinetic energy to generate thrust. For optimum performance, it is necessary to analyze the inlet and outlet pressure. The paper studies how the nozzle operates under different outlet pressure (back-pressure) conditions while keeping the inlet pressure constant at 50 bar. Analytical calculations were performed to predict the critical back-pressure, and it was found that a normal shock appears in the nozzle when the back-pressure lies between 9.49 and 49.74 bar. Optimal expansion is achieved when the back-pressure is approximately 0.684 bar, corresponding to a supersonic Mach number of 3.47. These analytical predictions are compared with CFD simulations performed in ANSYS Fluent using the SST k–ω turbulence model. Shock waves were observed at 45, 35, and 15 bar back-pressure, while at 5 bar the flow was fully expanded and shock-free. The maximum Mach numbers obtained numerically for the respective back-pressures were 0.826, 1.318, 2.35, and 2.4. The percentage deviations from the ideal analytical Mach number (3.47) were 76.2%, 62.0%, 32.3% and 30.5%, respectively. The results indicate that increasing the pressure ratio between the inlet and backpressure shifts the shock wave towards the outlet of the nozzle and ultimately eliminates it at sufficiently low pressure. This work directly quantifies shock location and Mach number deviations from ideal isentropic theory by plotting a graph of Mach number along the centerline.

Keywords
CD nozzle, backpressure, shock wave, CFD analysis

1. Introduction

The main purpose of designing a CD nozzle is to accelerate a compressible fluid to supersonic speeds. A CD nozzle consists of three sections: a converging, a throat, and a diverging section. As the cross-sectional area gets smaller in the converging section, the speed slowly goes up and the pressure slowly goes down. The fluid reaches the speed of sound (Mach 1) at the throat, which is the minimum-area section of the nozzle. Beyond the throat, the diverging section allows the flow to accelerate to supersonic speeds (Mach > 1) (Chaudhary 2024).

These types of nozzles are used in propulsion systems such as rockets and supersonic jets. For use in steam turbines, the convergent-divergent (CD) nozzle was first developed independently by Ernst Körting in 1878 and later by the Swedish inventor Gustaf de Laval in 1888. This nozzle design was later adopted by Robert Goddard. For rocket propulsion, every rocket engine is designed to transform subsonic flow into higher-speed flow. In this design, the convergent section accelerates subsonic flow up to sonic speed once a specific pressure ratio is reached, a state known as choked flow (Vadivelu et al. 2022). Shock waves form when the backpressure is not sufficiently low to sustain a fully isentropic expansion of the supersonic flow. The presence of a shock wave causes a sudden rise in pressure and drop in velocity, reducing nozzle efficiency. In the late 1800s, Rankine and Hugoniot wrote about this phenomenon in an analytical way. For nozzle design to operate efficiently under various conditions, understanding shock behavior is crucial (Yang et al. 2025). The back-pressure of the CD nozzle directly influences the flow structure within the divergent section (Chen et al. 2022).

This numerical and analytical study highlights the relationship between back-pressure variations and flow development inside a CD nozzle, visualizing the formation (Vadivelu et al. 2022). Apart from theoretical modeling, practical nozzles often show deviations in Mach numbers from expected values due to real-world effects such as viscous losses and turbulence.

1.1 Objectives

This study implies that, based on an inlet pressure of 50 bar, the outlet Mach number is 3.47 for the supersonic region and 0.0849 in the subsonic region, with corresponding pressures of 0.684 bar and 49.74 bar, respectively. For the numerical analysis, ANSYS Fluent was used with the SST k-ω turbulence model to achieve better accuracy (Al-Rbaihat et al. 2023). Four back-pressure conditions (45, 35, 15, and 5) were simulated to examine shock-wave formation.

Specifically, shock waves appear at back-pressures of 45, 35, and 15 bar, whereas at 5 bar, the flow expands fully into a supersonic state without shock formation. The Mach number and pressure along the centerline graph and the Mach number and pressure contour for the CD of the nozzle were analyzed.

Future studies may include the exploration of transient shock dynamics, three-dimensional flow behavior, and advanced turbulence-model analysis.

1.2 Contributions

The main contributions of this study are:

- Establishing a detailed correlation between analytically predicted shock formation and 2CFD results in a conical CD nozzle at a fixed inlet pressure of 50 bar for four back-pressures (45, 35, 15, and 5 bar)
- Comparing the analytical and CFD Mach numbers and shock locations in numbers, and then calculating the percentage differences from the ideal exit Mach number for each back-pressure case.
- Showing how decreasing back-pressure moves the shock toward the outlet and eventually fades out, presenting helpful details on how to control back-pressure and how nozzle performance can decrease.

2. Literature Review

Early works indicate that the discontinuities of pressure and velocity in the diverging section of a convergent-divergent (CD) nozzle are caused by shock waves (Kim, Matsuo, and Setoguchi 1996). When the back-pressure is sufficiently high with respect to the inlet pressure, normal or oblique shock waves are formed in the diverging section, resulting in a sudden loss of velocity or Mach number and an increase in pressure that affects the nozzle efficiency. Experimental studies and simulations consistently document these shock waves (He, Qin, and Liu 2015).

Back-pressure is the main driver in nozzle flow, determining whether the flow remains fully supersonic or forms shock. Computational and experimental studies have demonstrated that as back-pressure increases for a constant inlet pressure, the location of the shock wave moves upstream within the diverging section. Conversely, lowering the back-pressure allows the flow to expand fully, producing the highest possible Mach number at the exit of the CD nozzle (Gillespie and Sandham 2022).

Nozzle shapes, diverging angles, and throat geometry play a critical role in where and how shock waves develop. For example, certain rectangular nozzles can produce higher exit Mach numbers and increased pressure compared to the circular or square designs. Optimizing nozzle geometry alongside operating parameters is essential for maximizing the thrust and minimizing the shock wave formation in a converging-diverging nozzle (Sabnis et al. 2022).

Using CFD (Computational Fluid Dynamics) with turbulence models like SST k-ω in ANSYS Fluent has provided a more accurate prediction of boundary layer behavior, shock location, and separation phenomena in the CD nozzle. Modern studies combine experimental and computational data to obtain more accuracy. Such hybrid approaches have clarified real-world effects and improved understanding of the gap between theory and practice (Unnikrishnan and Vasantakumar 2020).

Extensive research has analyzed shock formation and flow characteristics in CD nozzles using both analytical and numerical methods (Yang et al. 2025) (Nagata et al. 2020).

Previous studies have thoroughly investigated that shocks in CD nozzles cause pressure and velocity discontinuities depending on back-pressure, geometry, and viscous and turbulent effects, often using back-pressure, geometry, and viscous and turbulent effects. They address various configurations and objectives rather than a single, tightly defined operating case.

The present work focuses on a single conical CD nozzle with a fixed inlet pressure of 50 bar and four specific back-pressures to quantify how shock location and Mach number deviate as back-pressure changes. This focused analytical-numerical correlation for a single conical geometry and defined pressure range is not covered in the cited works. This approach thus offers a more direct, design-oriented view of how actual viscous and turbulent effects alter shock behavior and performance in a practical CD nozzle.

3. Methodology

This study refers to an analytical and numerical approach to investigate shock wave formation. At first theoretical calculations are performed based on governing equations, and then they are compared with CFD predictions.

3.1 Design of CD Nozzle

This study refers to an analytical and numerical approach to investigate shock wave formation. At first theoretical calculations are performed based on governing equations, and then they are compared with CFD predictions (Table 1).

Table 1. Details of the CD Nozzle

Segment	Dimensions
Inlet diameter	40 mm
Outlet diameter	80 mm
Throat Diameter	30.60 mm
Convergent length	40 mm
Divergent length	170 mm
Converging angle	6.7 degrees
Diverging angle	8.27 degrees

A detailed schematic diagram of the convergent-divergence nozzle is in Figure 1. Both analytical and numerical analyses utilize the dimensions of the inlet, throat, and exit, as illustrated in the diagram.

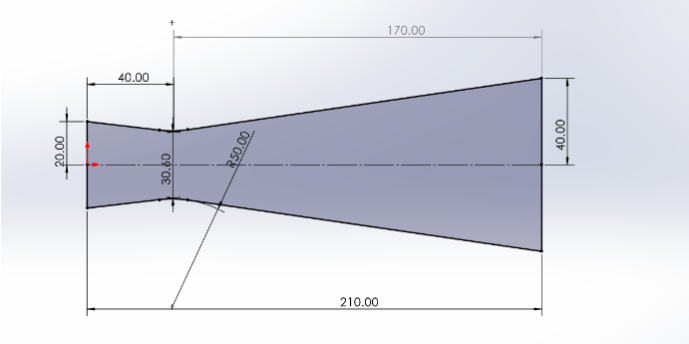

Figure 1. Nozzle Diagram

3.2 The Governing Equations

The compressible flow in a convergent-divergent nozzle is based on the fundamental conversion equation of mass, momentum, and energy (theoretical analysis). The flow should be steady, adiabatic, one-dimensional, and an ideal gas (Angielczyk 2025).

The **continuity equation** ensures the conservation of mass:

$$\dot{m} = \rho A V = constant \tag{1}$$

The **continuity equation** ensures the conservation of mass:

$$h + \frac{V^2}{2} = h^0 = constant \tag{2}$$

For an ideal gas, the relationship between static and total temperatures is defined as follows:

$$T^0 = T\left(1 + \left(\frac{\gamma - 1}{2}\right)M^2\right) \tag{3}$$

Combining the continuity and energy equations provides the **area–Mach number relation** for isentropic flow:

$$\frac{A}{A^*} = \left(\frac{1}{M}\right)\left[\frac{2}{\gamma+1}\left(1 + \frac{\gamma-1}{2} * M^2\right)\right]^{\frac{\gamma+1}{2*(\gamma-1)}} \tag{4}$$

The **pressure ratio** relationship for isentropic flow is expressed as:

$$\frac{P}{P} = \left[1 + \frac{\gamma-1}{2} * M^2\right]^{-\frac{\gamma}{\gamma-1}} \tag{5}$$

These equations form the foundation for analytical prediction of pressure, temperature, and Mach number variations inside the nozzle.

3.3 Analytical Method

The governing equation (1)-(5) is used to determine flow characteristics along the nozzle. The analysis of shock wave formation in the CD nozzle used the exit-to-throat area ratio (Ae/A*) (Table 2).

Table 2. Parameters used in calculation

Parameter	Value
Throat diameter	30.6 mm
Exit Diameter	80 mm
A	5026.5 mm^2
A*	735.4 mm^2
A/A*	6.835
γ	1.4 (air)
Inlet pressure	50 bar

3.3.1 Mach Number Determination

The exit-to-throat ratio A/A* = 6.835 and specific heat ratio $\gamma = 1.4$ are substituted into the isentropic area- Mach relation (Eq.4). This leads to the cubic in Mach number

$$M^2 + 5 - 11.3839M^{\frac{1}{3}} = 0 \quad (7)$$

Eq. 7 can be solved using established analytical or numerical methods. For A/A* > 1, the area-Mach relation always produces two real positive solutions corresponding to a subsonic and a supersonic branch shown in Table 3.

Table 3. Region

Region	Mach number
Subsonic	0.0849
Supersonic	3.47

3.3.2 Back-pressure Determination

Once Mach numbers are determined, Eq. (5) is applied to calculate the corresponding back-pressures. For the supersonic region (M = 3.47), the back-pressure is 0.684 bar. For a perfectly expanded nozzle, the back-pressure is 0.684 bar.

Similarly for the supersonic region (M = 0.0849), the back-pressure is 49.74 bar.
Therefore, the nozzle is choked for all the backpressure below 49.74 bar.

3.3.3 Range for Shock wave formation

From Normal Shock table for M = 3.47

$$P_2 / P_1 = 13.881$$

$$P_2 = 13.8811 \times 0.684$$

$$P_2 = 9.49\ bar$$

P_2 = Minimum back-pressure for creating normal shock

P_1 = Back-pressure for perfect expansion (0.684 bar)

Therefore, Normal shock will appear in the nozzle over the range of 9.49 bar to 49.74 bar.

Table 4 summarizes the key analytical predictions of Mach number and pressure for the CD nozzle.

Table 4. Analytical nozzle results

Region	Mach numbers	Static Pressure (bar)
Subsonic	*0.0849*	*49.74*
Supersonic	*3.47*	*0.684*
Shock min	-	*9.49*
Choked max	-	*49.74*

3.4 Numerical Method

The current work involves performing CFD simulations to numerically validate the analytical method developed. A detailed flowchart is provided to illustrate the numerical solution procedure for better understanding.

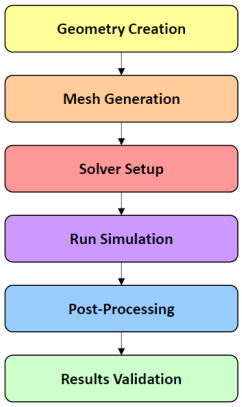

3.4.1 Modeling the CD Nozzle

The two-dimensional model of the CD nozzle is modeled with the help of SolidWorks 2022, as shown in Figure 2.

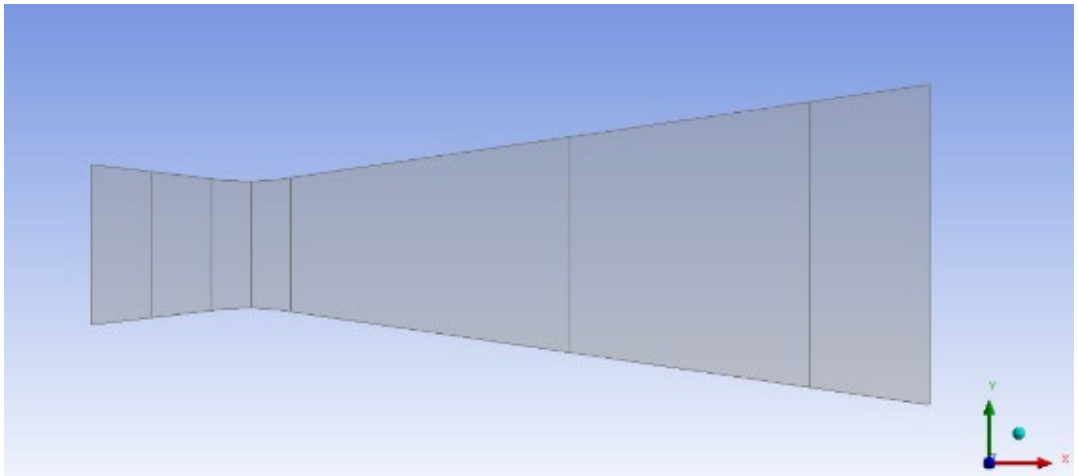

Figure 2. 2D Model of nozzle

3.4.2 Meshing

For meshing, ANSYS Workbench (fluid flow-fluent) was used. The key mesh parameters used in the simulation are summarized in Table 5.

Table 5. Computational Grid Parameters

Parameter	Value
Element Type	Quadrilateral
Number of Elements	9796
Number of Nodes	10000
Element Size	11.236 mm
Growth Rate	1.2
Solver Type	Pressure-Based
Meshing Tool Used	ANSYS Workbench Meshing

The detailed mesh generation is shown in Figure 3.

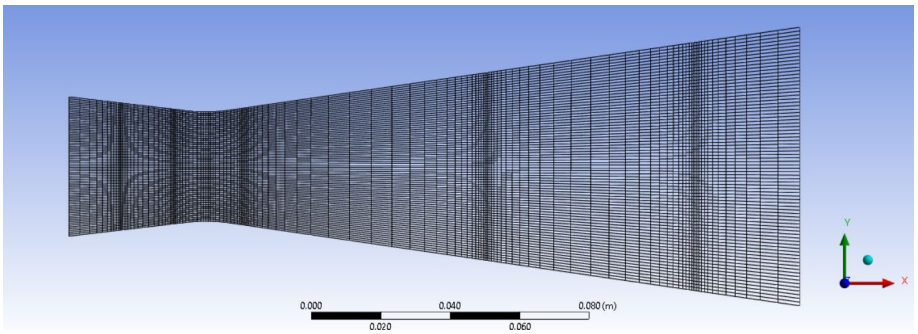

Figure 3. Generated Mesh CD nozzle

3.4.2.1 Mesh Dependency Test

A mesh refinement study was conducted on the CD nozzle geometry to determine the optimal mesh density and ensure an accurate solution. The results are presented in Figure 4, which shows the mesh dependency curve for the CD nozzle where the maximum Mach number (for back-pressure 5 bar) is plotted against element count. At low mesh densities, the Mach numbers vary noticeably. After 4000-5000 elements, the curve becomes almost flat, indicating mesh independence.

The selected mesh of 9796 elements lies within this stable region, where further refinement produces negligible changes in Mach numbers.

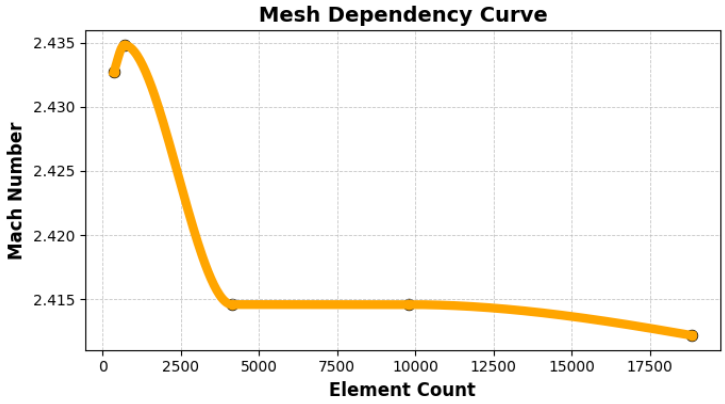

Figure 4. Mesh dependency Curve

3.4.3 Solver Setup

The meshed model is imported in ANSYS FLUENT. A pressure-based solver is used for the analysis. Gravity is not considered. Energy is enabled for temperature calculations, and the viscous model used is **SST K-Omega**. A detailed overview is shown in Table 6 and Table 7.

Table 6. Properties of gas

Parameter	Value	Units
Gama for gas	1.4	-
Thermal Conductivity	0.0242	W/(m·K)
Specific Heat (Cp)	1006.43	J/(kg·K)
Viscosity	1.7894 e-05	kg/(m·s)
Molecular Weight	28.966	kg/kmol
Density	Ideal gas	-

Table 7. Boundary Conditions

Symbol	Type	Value
Nozzle Inlet	*Pressure-inlet*	*50 bar*
Outlet	*Pressure-outlet*	*45, 35, 15, 5 bar*
Inlet Temperature	-	*1500 K*
Outlet Temperature	-	*300 K*

After completing the solver setup, the solution was initialized. The number of iterations was set to 1000. All the residuals are observed to ensure the convergence. The solution had stabilized and was ready for post-processing.

3.5 Validation against Reference CD Nozzle Data

This study replicates the CD nozzle configuration and operating conditions reported in the reference work (Vadivelu et al. 2022) to compare Mach number distribution and shock location inside the nozzle. The same overall geometry inlet total pressure (80 bar), total temperature and perfect air model with $\gamma = 1.4$, along with ideal behavior are adopted to ensure that any differences arise primarily from numerical modeling rather than from boundary condition.

For these matched conditions, Mach number versus nozzle length curves along the centerline and corresponding flow-field contours were generated at the same set of backpressure values (70, 75 and 10 bar). These plots are used to assess the agreement in shock existence, shock position, and peak Mach number between the present simulations and the reference study (Table 8).

Table 8. Validation Comparison – Mach Number Distribution and Shock Position Against (Vadivelu et al. 2022)

Back-pressure (bar)	Inlet Pressure (bar)	Shock position (mm) – reference	Shock position (mm) – present work	Max Mach – reference	Max Mach – present work
75	*80*	*41.29*	*40.63*	*0.7459*	0.7420
70	*80*	*47.73*	*47.90*	*1.2698*	1.2269
10	*80*	*>165*	*>165*	*2.4132*	2.4082

The comparison in Table 6 demonstrates satisfactory agreement between the present CFD study and the reference work. At the back-pressures of 70 and 70 bar, the shock positions only differ by approximately 0.5 mm. And the maximum Mach numbers are within around 2% of the reference value.

These results validate the present solver and mesh for reliable analysis of shock behavior and Mach distribution in the CD nozzle.

Figure 5 shows the Mach number along the centerline for 75, 70, and 10 bar, indicating that both studies predict similar shock locations at higher back-pressures and nearly identical shock-free profiles at 10 bar.

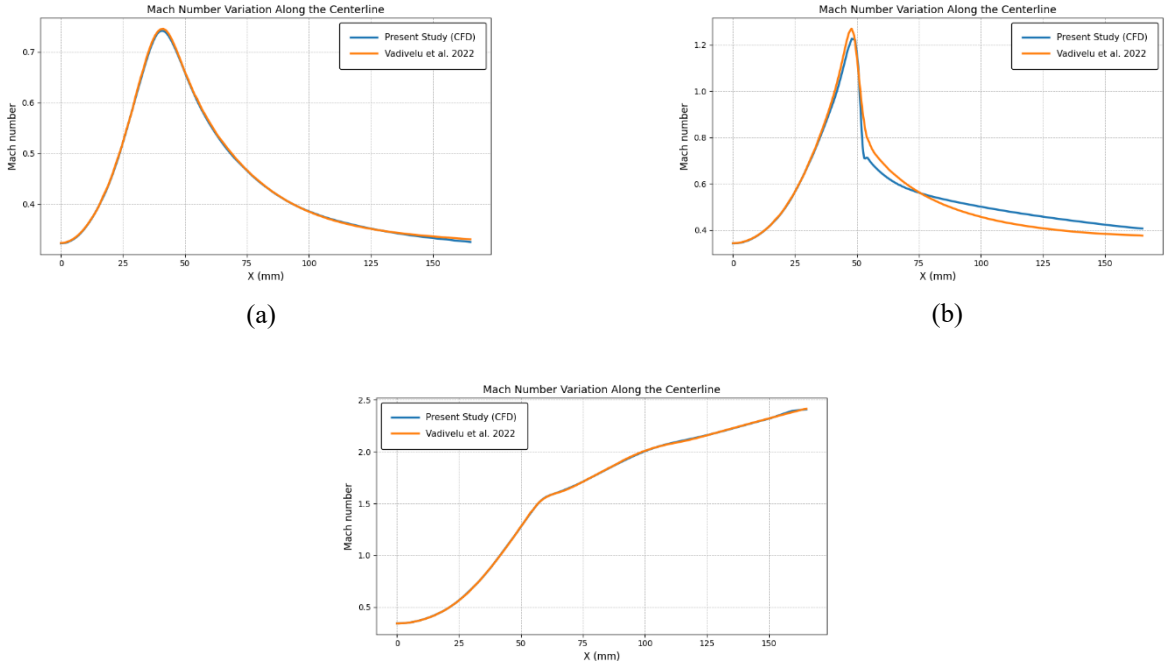

Figure 5. Validation of Mach Number Distribution Along the Centerline
(a) 75 bar, (b) 70 bar and (c) 10 bar back-pressure

4. Results and Discussion

The pressure difference between the inlet and outlet is important for creating flow. In this study, the inlet pressure was fixed at 50 bar throughout the analysis. To analyze the shock wave, CFD simulations are conducted for a range of back-pressures (5 bar, 15 bar, 35 bar, and 45 bar).

The result is presented in form of:

- **Mach Number**: Helps to highlight the shock wave formation and supersonic or subsonic region.
- **Pressure Contour**: Highlighting pressure variations

Graphical Plots:

- **Mach Number vs. Nozzle Length**: It helps to track the Mach Number along the centerline
- **Pressure vs. Nozzle Length**: Tracking static pressure along centerline.

From the analysis, results are shown in the form of contours (pressure, Mach number) and graphs (pressure along the centerline, Mach number along the centerline) to compare the CFD analysis (numerically) with the analytical method. The Result of various back-pressure are shown below.

4.1 Results for 45 and 35 bar back-pressure

At 45 bar and 35 bar backpressure, clear shock formation occurs by observing the instant pressure rise and Mach number drop. Figure 6 displays the Mach number and pressure contours obtained for 45 bar. The Mach number and pressure contours for 35 bar are shown in Figure 8. As per the analytical method, the shock waves appear if the back-pressure is above 9.49 bar. The flow is accelerated at the convergent section and then starts decelerating until the exit comes. In the case of 45 bar, this effect occurs because the high backpressure restricts flow expansion, forcing the supersonic region to terminate earlier and decelerate back to the subsonic region to satisfy the outer boundary. The CFD results for 35 bar match the analytical method, which shows that lowering back-pressure increases supersonic flow. The highest Mach number for 45 bar is close to the sonic region (M = 0.826), and the highest Mach number for 35 bar is close to the sonic region (M = 1.318). For both 35 bar and 45 bar, this pressure behaves oppositely to the Mach number. Graphs of Mach number along the centerline and pressure along the centerline for 45 bar back-pressure are shown in Figure 7, and for 35 bar back-pressure are shown in Figure 9. The graphic analysis remains consistent for both the backpressure and the contour. From the Mach number of the 45 bar back-pressure graph, it can be observed that the maximum Mach number occurs at a distance of 37 mm from the inlet along the centerline, and for 35 bar, it is observed that the maximum Mach number occurs at a distance of 55 mm from the inlet along the centerline, and the shock wave propagates toward the nozzle outlet.

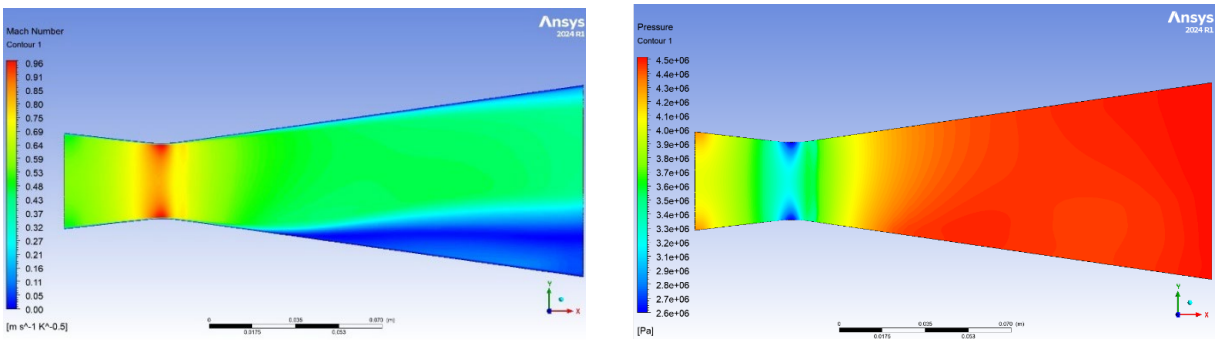

(a) (b)

Figure 6. (a) Mach number and (b) pressure contours for 45 bar back-pressure

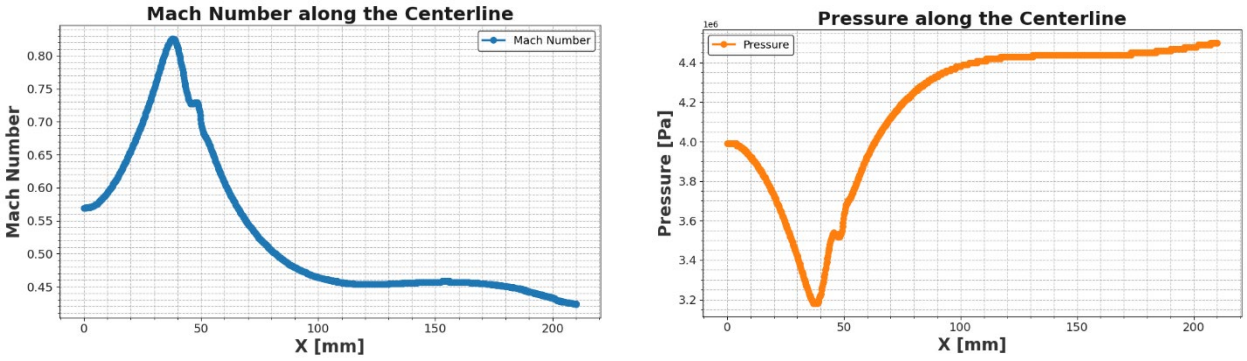

(a) (b)

Figure 7. (a) Mach number and (b) pressure along centerline for 45 bar back-pressure

4.2 Results for 15 bar back-pressure

At 15 bar back-pressure, continuous acceleration occurs due to the major pressure difference between the inlet and outlet, resulting in stronger expansion and a larger supersonic region before the shock forms. As per the analytical

method, the shock waves appear if the back-pressure is above 9.49 bar. Unlike the 35 bar backpressure, the maximum Mach number is almost in the supersonic region (M = 2.35). Figure 10 displays the Mach number and pressure contours obtained for 15 bar, and Figure 11 shows the Mach number and pressure along the centerline. The Mach number graph reveals that the maximum Mach number happens at a distance of 191 mm from the inlet. These results align closely with the analytical prediction that shocks occur between 9.49 and 49.74 bar back-pressure, validating the CFD approach.

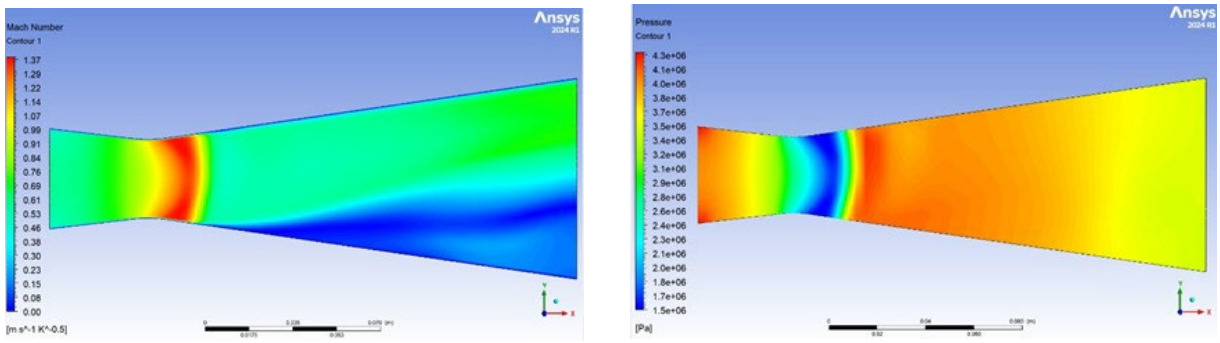

(a) (b)

Figure 8. Mach number(a) and pressure(b) contours for 35 bar back-pressure

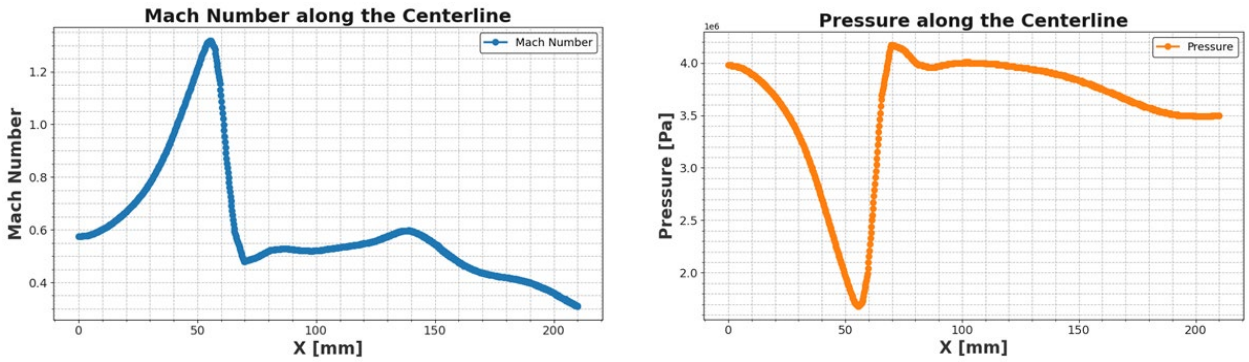

(a) (b)

Figure 9. Mach number(a) and pressure(b) along centerline for 35 bar back-pressure

4.3 Results for 5 bar back-pressure

In 5 bar, Pressure difference is more than the previous one, resulting continuous acceleration without shock formation. The pressure decreases continuously due to inverse relationship with Mach number. As per the analytical method the Shock wave will not be appear if the back-pressure is below 9.49 bar, resulting in fully expanded supersonic flow reaches a maximum Mach number of 2.41. Mach Number and pressure contours obtained for 5 bar are shown in Figure 12, and Graph of Mach number along centerline and pressure along centerline are shown in Figure 13, confirm that no discontinuities are present. This case represents the optimal expansion condition maximizing nozzle efficiency.

Finally, it can be concluded that the analytical prediction of shock wave formation is in good agreement with the numerical results, considering the effects of viscosity and turbulence.

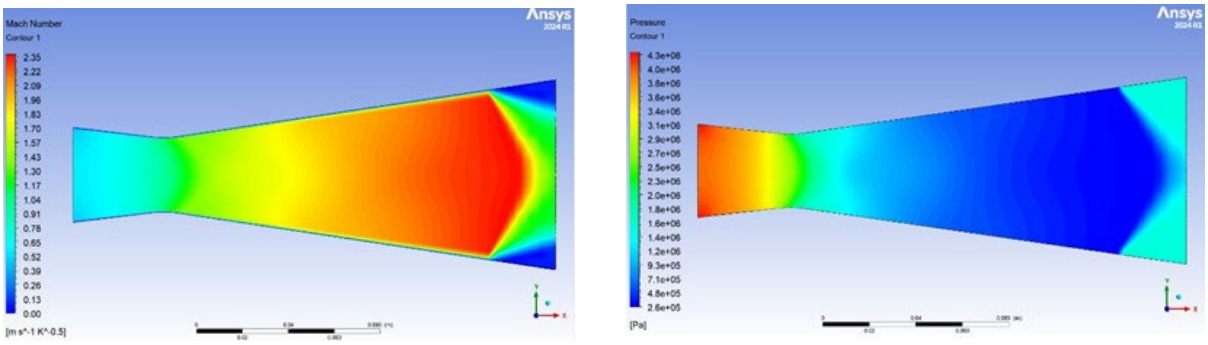

(a) (b)

Figure 10. (a) Mach number and (b) pressure contours for 15 bar back-pressure

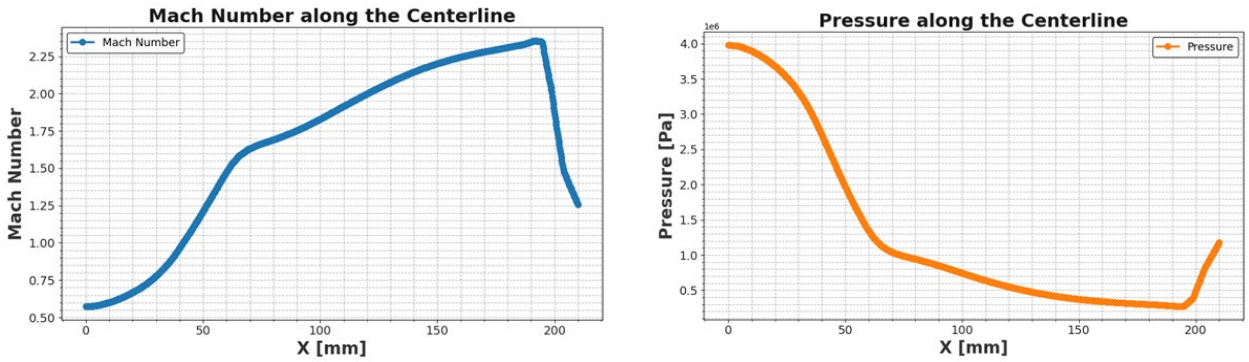

(a) (b)

Figure 11. (a) Mach number and (b) pressure along centerline for 15 bar back-pressure

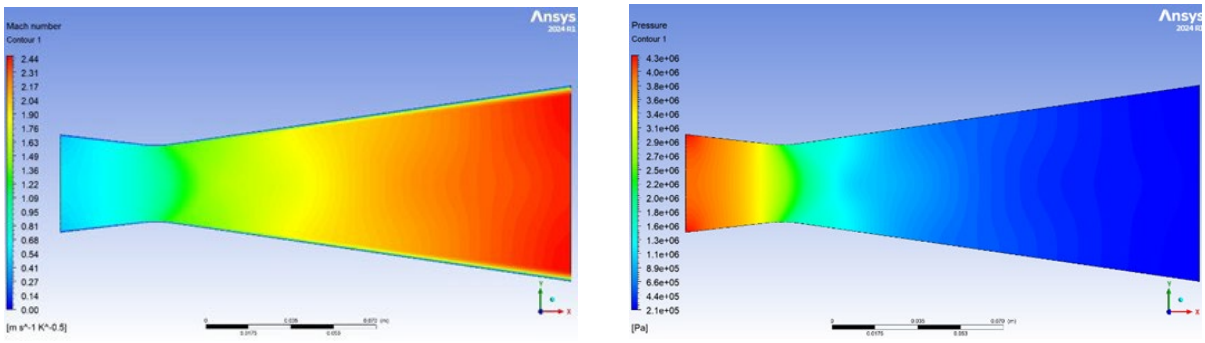

(a) (b)

Figure 12. (a) Mach number and (b) pressure contours for 5 bar back-pressure

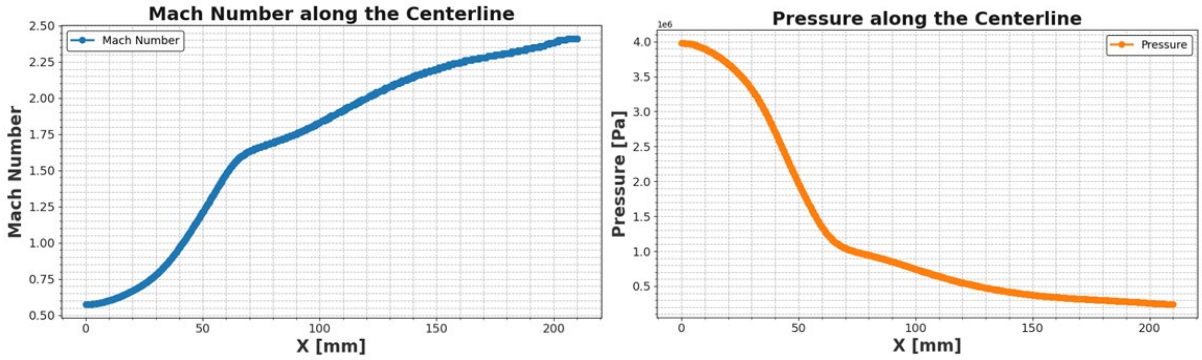

(a) (b)

Figure 13. (a) Mach number and (b) pressure along centerline for 5 bar back-pressure

4.4 Summary of Results and Correlation

Shocks were observed at the back-pressure of 45, 35, and 15 bar, while at 5 bar the flow became fully expanded and shock-free. The maximum Mach numbers obtained numerically for the respective back-pressures were 0.826, 1.318, 2.35, and 2.4. Due to viscous and turbulent effects, the percentage deviations from the ideal analytical Mach number (3.47) were 76.2%, 62.0%, 32.3%, and 30.5%.

Table 9 compares analytical and numerical Mach numbers. Table 9 displays the shock positions for each backpressure, along with the corresponding percentage deviations.

Table 9. Boundary Conditions

Back-pressures (bar)	Analytical Exit Mach	CFD Max Mach	Errors in Mach (%)	Shock position from inlet (mm)
45	*3.47*	*0.826*	*76.2*	*37*
35	*3.47*	*1.318*	*62*	*55*
15	*3.47*	*2.35*	*32.3*	*191*
5	*3.47*	*2.40*	*30.5*	*No internal shock*

The numerical results demonstrate that the relationship between shock wave formation and back-pressure is inversely correlated. Higher back-pressure (45 bar) means the shock wave forms close to the throat. And with sufficiently low back-pressure (below 9.49, such as 5 bar), no shock wave forms. The flow is fully expanded and entirely supersonic. Due to the reduction in backpressure, the expansion ratio is increased, shifting the normal shock toward the outlet of the nozzle. The correlation between the CFD and analytical results confirms that both backpressure and nozzle shape can directly influence the formation of shock waves, which is impacting overall nozzle performance.

4.5 Significance and comparison with previous studies

Comparing with existing studies, similar behavior is reported. The position and strength of internal shock depend on the pressure ratio (back and inlet pressure) and complex flow structures of overexpanded nozzles (Hu et al. 2024). The practical Mach numbers found here are lower than ideal predictions due to viscous and turbulence effects (Restrepo and Simões-Moreira 2022).

5. Conclusion

Internal normal shocks were discovered by the analytical and numerical evaluation of a fixed-pressure (50 bar) conical convergent-divergent nozzle to be found between 9.49 and 49.74 bar. At 5 bar, the flow was considered fully expanded

and free from shock. The maximum CFD Mach numbers of 0.826, 1.318, 2.35, and 2.40 were obtained across the four simulated back-pressures (45, 35, 15, and 5 bar), respectively, which were significantly lower than the analytical supersonic exit Mach number of 3.47, showing the deviations of about 76.2%, 62.0%, 32.3%, and 30.5%. When back-pressure is decreased, the shock is pushed to a position further downstream towards the outlet, ultimately causing the shock to disappear from the nozzle outlet plane; thus, higher pressure ratios lead to larger supersonic regions, therefore yielding results conforming to ideal isentropic expectations.

Note that this study has multiple limitations. It only shows a two-dimensional model & one turbulence closure (SST k-ω), thereby neglecting the potential influence of three-dimensional effects, secondary flows, & sensitivity to turbulence modeling. Additionally, the uncertainty associated with boundary conditions, discretization errors, & the resolution of shocks is only partially characterized.

A mesh-dependency test was performed and indicated small sensitivity to further refinement, other numerical uncertainties (e.g., time independence, boundary-condition specification) are not fully quantified. In the future, the work should extend to fully three-dimensional nozzle geometries to show the 3D flow structures' influence on shock position and Mach number distribution, as well as to verify whether the trends observed here remain valid. By using transient simulations, we could investigate unsteady shock motion and possible shock oscillations for varying back-pressure. Furthermore, by comparing different turbulence models and more detailed uncertainty quantification, which includes finer mesh levels and specifications of alternative boundary conditions, we can improve confidence for practical nozzle design in the field of analytical–CFD correlation.

References

Al-Rbaihat, Raed, Khalid Saleh, Ray Malpress, David Buttsworth, Hussein Alahmer, and Ali Alahmer. “Performance Evaluation of Supersonic Flow for Variable Geometry Radial Ejector through CFD Models Based on DES-Turbulence Models, GPR Machine Learning, and MPA Optimization.” *International Journal of Thermofluids* 20. 2023.doi:10.1016/j.ijft.2023.100487.

Angielczyk, Wojciech. “Physical and Mathematical Problems of 1D Modelling of Transonic Two-Phase Flow in a Convergent-Divergent Nozzle.” *Archives of Thermodynamics* 46(1):141–54. 2025. doi:10.24425/ather.2024.152017.

Chaudhary, Pramod. “CFD Analysis of CD Nozzle with Sharp Throat and CD Nozzle with Curved Throat.” *Online Journal of Robotics & Automation Technology* 2(4). 2024. doi:10.33552/ojrat.2024.02.000542.

Chen, Changjiang, Yong Liu, Jiren Tang, and Huidong Zhang. “Effect of Nozzle Pressure Ratios on the Flow and Distribution of Abrasive Particles in Abrasive Air Jet Machining.” *Powder Technology* 397. 2022. doi:10.1016/j.powtec.2022.117114.

Gillespie, Alexander, and Neil D. Sandham. “Shock Train Response to High-Frequency Backpressure Forcing.” *AIAA Journal* 60(6):3736–48. 2022. doi:10.2514/1.J060811.

He, Miaosheng, Lizi Qin, and Yu Liu. “Numerical Investigation of Flow Separation Behavior in an Over-Expanded Annular Conical Aerospike Nozzle.” *Chinese Journal of Aeronautics* 28(4):983–1002. 2015. doi:10.1016/j.cja.2015.06.016.

Hu, Haifeng, Xinni Gao, Yushan Gao, and Jianwen Yang. “Shock Wave and Aeroelastic Coupling in Overexpanded Nozzle.” *Aerospace* 11(10). 2024. doi:10.3390/aerospace11100818.

Kim, H. D., K. Matsuo, and T. Setoguchi. “Investigation on Onset of Shock-Induced Separation.” *Shock Waves* 6(5):275–86. 1996. doi:10.1007/BF02535741.

Nagata, T., T. Nonomura, S. Takahashi, and K. Fukuda. “Direct Numerical Simulation of Subsonic, Transonic and Supersonic Flow over an Isolated Sphere up to a Reynolds Number of 1000.” *Journal of Fluid Mechanics* 904. 2020. doi:10.1017/jfm.2020.629.

Restrepo, Julián, and José R. Simões-Moreira. “Viscous Effects on Real Gases in Quasi-One-Dimensional Supersonic Convergent Divergent Nozzle Flows.” *Journal of Fluid Mechanics* 951. 2022. doi:10.1017/jfm.2022.853.

Sabnis, Kshitij, Daniel S. Galbraith, Holger Babinsky, and John A. Benek. “Nozzle Geometry Effects on Supersonic Wind Tunnel Studies of Shock–Boundary-Layer Interactions.” *Experiments in Fluids* 63(12). 2022.doi:10.1007/s00348-022-03543-1.

Unnikrishnan, Jijo, and Vyshnav Vasantakumar. *Experimental and Computational Analysis of Shock Structure in a Supersonic Contoured Nozzle*. www.ijert.org. 2020.

Vadivelu, P., G. Senthilkumar, G. Sivaraj, D. Lakshmanan, and Nayani Uday Ranjan Goud. “Performance Analysis of CD Nozzle.” Pp. 620–31 in *Materials Today: Proceedings*. Vol. 64. 2022. Elsevier Ltd.

Yang, Yi, Qiancheng Wang, Yuxin Zhao, Gang He, and Yilong Zhao. "Unsteady Shock Wave Behaviors in Supersonic Nozzle Exit under Varying Over-Expanded Conditions." *Physics of Fluids* 37(8):086160. 2025.doi:10.1063/5.0283192.